Antiviral Research 79 (2008) 19–27

Contents lists available at ScienceDirect

Antiviral Research

journal homepage: www.elsevier.com/locate/antiviral

Synthesis of 1-β-D-ribofuranosyl-3-ethynyl-[1,2,4]triazole and its *in vitro* and *in vivo* efficacy against *Hantavirus*

Dong-Hoon Chung[a], Sidath C. Kumarapperuma[b], Yanjie Sun[a], Qianjun Li[a], Yong-Kyu Chu[a], Jeffrey B. Arterburn[b], William B. Parker[a], Jeffrey Smith[c], Kristin Spik[c], Harish N. Ramanathan[d], Connie S. Schmaljohn[c], Colleen B. Jonsson[a,*]

[a] *Department of Biochemistry and Molecular Biology, 2000 9th Avenue South, Southern Research Institute, Birmingham, AL 35205, United States*
[b] *Department of Chemistry and Biochemistry, New Mexico State University, Las Cruces, NM 88003, United States*
[c] *United States Army Medical Research Institute of Infectious Diseases, Ft. Detrick, MD 21703, United States*
[d] *Department of Biochemistry, University of Alabama, Birmingham, AL 35205, United States*

ARTICLE INFO

Article history:
Received 2 November 2007
Accepted 20 February 2008

Keywords:
Hemorrhagic fever with renal syndrome
HFRS
Hantaan virus HTNV
Andes virus
Ribavirin
Crimean Congo hemorrhagic fever virus
Rift Valley fever virus

ABSTRACT

There are no FDA approved drugs for the treatment of hemorrhagic fever with renal syndrome (HFRS), a serious human illnesses caused by hantaviruses. Clinical studies using ribavirin (RBV) to treat HFRS patients suggest that it provides an improved prognosis when given early in the course of disease. Given the unique antiviral activity of RBV and the lack of other lead scaffolds, we prepared a diverse series of 3-substituted 1,2,4-triazole-β-ribosides and identified one with antiviral activity, 1-β-D-ribofuranosyl-3-ethynyl-[1,2,4]triazole (ETAR). ETAR showed an EC_{50} value of 10 and 4.4 μM for Hantaan virus (HTNV) and Andes virus, respectively. ETAR had weak activity against Crimean Congo hemorrhagic fever virus, but had no activity against Rift Valley fever virus. Intraperitoneally delivered ETAR offered protection to suckling mice challenged with HTNV with a ~25% survival at 12.5 and 25 mg/kg ETAR, and a MTD of 17.1 ± 0.7 days. ETAR was phosphorylated in Vero E6 cells to its 5′-triphosphate and reduced cellular GTP levels. In contrast to RBV, ETAR did not increase mutation frequency of the HTNV genome, which suggests it has a different mechanism of action than RBV. ETAR is an exciting and promising lead compound that will be elaborated in further synthetic investigations as a framework for the rational design of new antivirals for treatment of HFRS.

1. Introduction

Despite efforts to develop vaccines and antiviral drugs, effective therapeutics for treatment of most hemorrhagic fever viruses remain largely unavailable (Andrei and De Clercq, 1993; Bangash and Khan, 2003; Bronze and Greenfield, 2003; De Clercq, 2005; Maes et al., 2004). Hantaviruses are globally distributed and several members of the genus cause deadly human illnesses such as hemorrhagic fever with renal syndrome (HFRS) or hantavirus pulmonary syndrome (HPS) (Schmaljohn and Hjelle, 1997). Old World hantaviruses, Hantaan virus (HTNV) and Puumala virus, are responsible for most HFRS cases in Asia and Europe, whereas the New World hantaviruses, Sin Nombre virus (SNV) and Andes virus (ANDV), are responsible for the majority of HPS cases in North and South America, respectively (Peters et al., 1999). In striking contrast to all other HPS and HFRS-causing viruses (Vitek et al., 1996; Wells et al., 1997), ANDV represents the first hantavirus associated with person-to-person transmission in Argentina and Chile (Chaparro et al., 1998; Enria et al., 1996; Lopez et al., 1996; Martinez et al., 2005; Padula et al., 1998). While ribavirin (RBV; 1-β-D-ribofuranosyl-1,2,4-triazole-3-carboxamide) has shown efficacy in treating HFRS patients in China (Huggins et al., 1991), its potential efficacy is still unknown for HPS cases (Chapman et al., 1999; Mertz et al., 2004).

In addition to *Hantavirus*, several other genera in the family *Bunyaviridae* cause hemorrhagic fever disease in humans. Crimean Congo hemorrhagic fever virus (CCHFV) and Rift Valley fever virus (RVFF) reside in the *Nairovirus* and *Phlebovirus*, respectively, and have mortality rates from 1% (RVFV) to 5-40% (CCHFV). Hantaviruses are enzootic viruses of wild rodents and cause persistent infections without apparent disease symptoms in their natural hosts (Botten et al., 2000; Botten et al., 2002; Compton et al., 2004; Lee et al., 1981; Yanagihara et al., 1985). However, the basic genome structure and replication cycles of members of the family *Bunyaviridae* share many similarities (Schmaljohn and Hooper, 2001), and therefore, antiviral drugs may prove effective for more

* Corresponding author. Tel.: +1 205 581 2681; fax: +1 205 581 2093.
E-mail address: Jonsson@sri.org (C.B. Jonsson).

0166-3542/$ – see front matter © 2008 Elsevier B.V. All rights reserved.
doi:10.1016/j.antiviral.2008.02.003

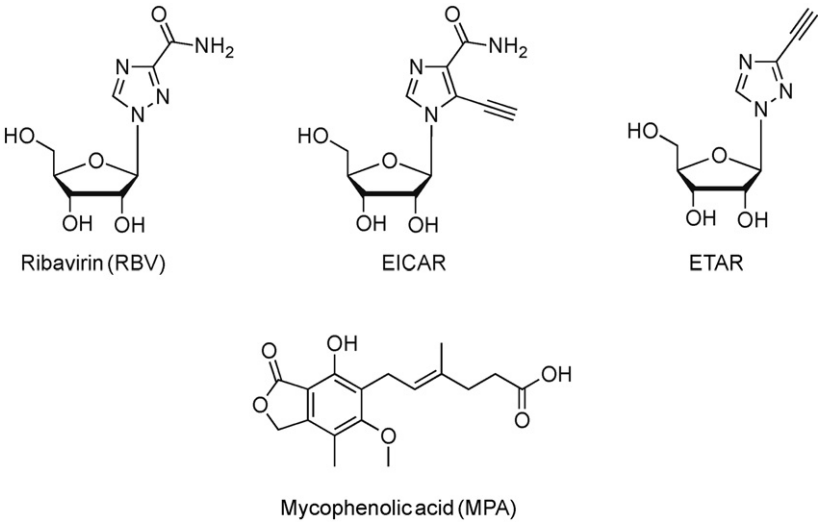

Fig. 1. Structures of RBV, MPA, EICAR, and ETAR.

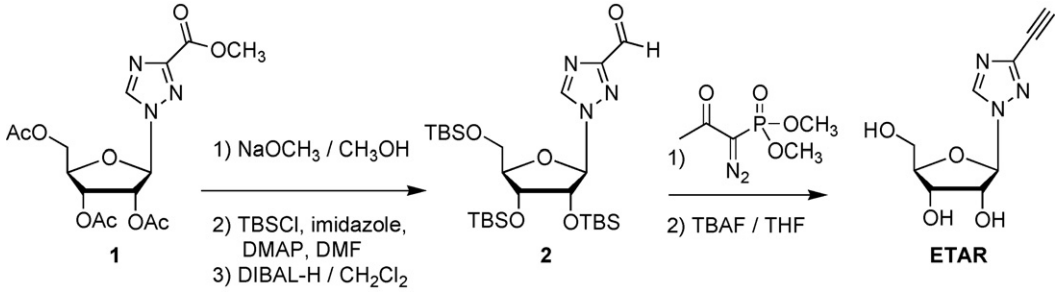

Scheme 1. Synthesis of ETAR.

than one genus. All the *Bunyaviridae* have three negative-sense, single-stranded RNA segments (S, M, and L), which encode the nucleocapsid (N), two glycoproteins (G_N and G_C) and the L protein, respectively (Schmaljohn and Hooper, 2001; Schmaljohn et al., 1983). The L protein or RNA dependent RNA polymerase (RdRp) mediates both the replication of the genomic and anti-genomic viral RNAs and the transcription of viral mRNAs in the cytoplasm. The conservation of function across RNA polymerases suggests that broad spectrum nucleoside antivirals may be identified that act across genera in the *Bunyaviridae*.

Nucleoside analogs have been identified that acted on several members of the *Bunyaviridae*, albeit with differential levels of activity (Sidwell et al., 1972). The driving mechanism(s) underlying one of these drugs, RBV, has been difficult to capture primarily due to its ability to interact with both host and viral targets. For example, RBVs' activity against HTNV did not correlate with inhibition of inosine monophosphate dehydrogenase (IMPDH), but rather with production of RBV triphosphate (RBV-TP) (Sun et al., 2007) and an increase in mutation frequency (Severson et al., 2003). We hypothesized that the increase in resulting mutation frequency is due to the incorporation of RBV by the L protein into the viral RNAs (Severson et al., 2003). These findings led us to explore chemical modifications that would increase selectivity and activity of RBV-based scaffolds toward the L protein.

Focusing on the heterocyclic-β-riboside structure, we prepared a diverse series of 3-substituted 1,2,4-triazole-β-ribosides, including isosteric derivatives of RBV and linkage isomers that exhibit altered hydrogen-bonding capacity. We have previously evaluated representative compounds from this series as substrates for adenosine kinase (Kumarapperuma et al., 2007). Herein, we describe the antiviral activity of 1-β-D-ribofuranosyl-3-ethynyl-[1,2,4]triazole (ETAR, Fig. 1) against 4 viruses, HTNV, ANDV, CCHFV, and RVFV. ETAR showed promising antiviral activity against HTNV, ANDV, and CCHFV, but not RVFV. Furthermore, it protected suckling mice from infection with HTNV to a degree that was similar to that seen with RBV.

2. Methods and materials

2.1. Chemistry and synthesis

The synthetic approach for the preparation of ETAR is shown in Scheme 1. Deacetylation of commercially available 1-(2,3,5-tri-*O*-acetyl-β-D-ribofuranosyl)-1*H*-1,2,4-triazole-3-carboxylic acid, methyl ester **1** with $NaOCH_3$ (72%), protection with *tert*-butyldimethylsilyl chloride (TBSCl) (67%), followed by selective reduction of the ester with 2.5 equivalents of diisobutylaluminium hydride (DIBAL-H) gave the triazole aldehyde **2** (75%). The aldehyde was converted to the alkyne with Bestmann's reagent (78%) (Goundry et al., 2003). The TBS groups were removed with tetrabutylammonium fluoride (TBAF) and the product was recrystallized from 5% CH_3OH in dichloromethane to obtain pure ETAR as a crystalline powder (90%). Spectroscopic and mass spectrometric characterization data for ETAR are provided.[1] Com-

[1] ETAR compound characterization: mp 174–175 °C; FT-IR peaks (cm^{-1}) 2130. 1H NMR (200 MHz, CD_3OD) δ 8.72 (s, 1H), 5.84 (d, 1H, $J_{1',2'}$ = 3.5 Hz, H-1′), 4.43 (m, 1H, H-2′), 4.29 (m, 1H, H-3′), 4.09 (m, 1H, H-4′), 3.83–3.79 (dd, 1H, $J_{5'a,5'b}$ = 12.3 and $J_{5'a,4'}$ = 3.3 Hz, H-5a), 3.73 (s, 1H), 3.70–3.65 (dd, 1H, $J_{5'b,5'a}$ = 12.9 and $J_{5'b,4'}$ = 4.7 Hz,

plete experimental details for the synthesis will be published elsewhere.

2.2. Viruses, cell culture, antibodies and inhibitors

All work with viruses was performed in biosafety level 3 (BSL3) containment according to CDC guidelines. HTNV (strain 76-118), ANDV (strain Chile-9717869, from T. Ksiazek, CDC, Atlanta), CCHFV IbAr 10200, and RVFV ZH501 were used for all experiments. Vero E6 cells (ATCC CRL 1586) were maintained in complete DMEM (Dulbecco's modified Eagle's medium supplemented with 10% fetal bovine serum, 1% penicillin–streptomycin (PS) and 1% L-glutamine). RBV was purchased from MP Biomedicals (USA). Mycophenolic acid (MPA) and guanosine were obtained from Sigma–Aldrich Co. (St. Louis, USA). Mono- and polyclonal antibodies against hantaviruses were prepared as described elsewhere (Ramanathan et al., 2007).

2.3. Determination of the effect of drug treatment on production of infectious virus

To measure the levels of infectious virus being released by cells in the presence of drug or mock controls we used a focus forming unit (FFU) assay and/or the standard plaque assay as described (Chung et al., 2007). Briefly, 3-day-old Vero E6 cells were grown in a six-well cell culture plate and infected with either HTNV or ANDV at a multiplicity of infection (moi) of 0.1 by adsorption for 60 min at 37 °C in 5% CO_2. After adsorption, the supernatant was removed and 2.5 mL of complete DMEM with the test compound was added (0.5% DMSO final concentration). After 3 days, the cell supernatant was harvested and measured for the presence of infectious hantavirus. The infectious progeny virus in the cell supernatant was evaluated as FFU as described previously (Ramanathan et al., 2007).

The anti-HTNV inhibitory activity was measured with a cell-based ELISA. In this assay, HTNV N protein levels were measured in the presence of compounds. Briefly, Vero E6 cells were seeded in 96-well cell culture plate and grown for 36 h. Cells were infected with HTNV by adsorption for 1 h at 0.1 moi. The supernatant was removed and 100 μL of a complete DMEM with serially diluted drug samples was added. Plates were incubated for 3 days and immunostained as follows. Cells were fixed with methanol:acetone (3:1) and washed with PBST (phosphate buffered saline with Triton X-100, 0.1%). HTNV N was detected by incubating the fixed cells on 96-well plate with HTNV N monoclonal antibody E-314 and HRP conjugated anti-mouse IgG. The murine monoclonal (E-314) was raised to HTNV N by Cell Essentials, Inc. (Boston, MA) as previously described (Chung et al., 2007). The color was developed with TMB substrate (SureBlue TMB 1-Component Microwell Peroxidase Substrate®, KPL), the colorization was stopped by the addition of TMB Stop Solution (KPL) to each well, and the intensity of developed color was measured at 450 nm wavelength using a PerkinElmer Envision™ plate reader (PerkinElmer, Wellesley, MA). The color intensity and the drug concentration were used to calculate EC_{50} using a Standard Curve Assay Analysis module of SigmaPlot software (Systat software Inc.).

Measurement of the levels of infectious RVF or CCHF virus being released by cells in the presence of ETAR was done as follows. Three-day-old Vero E6 cells were grown in six-well cell culture plates and infected with either RVFV ZH501 or CCHF IbAr 10200 at a moi of 0.1 by adsorption for 90 min at 37 °C in 5% CO_2 with rocking every 30 min. After adsorption, the supernatant was removed, the wells washed with PBS, and 2.0 mL of complete EMEM with 30 μM ETAP was added. After 3 days, the cell supernatants were harvested and analyzed for the presence of infectious RVFV or CCHFV by plaque assay. Briefly, 10-fold serial dilutions of the supernatants were prepared in either HBSS + 5% FBS (RVFV) or EMEM + 10% FBS (CCHFV). One hundred or two hundred microliters of dilution were added to 3-day-old Vero (RVFV) or Vero E6 (CCHFV) cells. Adsorption was for one h at 37 °C and 5% CO_2 with gentle rocking every 15 min. Two to three mL of primary overlay consisting of 0.6% SeaKem ME + 10% FBS in 2× EMEM was added, and the plates were incubated for 3 days at 37 °C and 5% CO_2. A secondary overlay consisting of 0.6% SeaKem ME + 5% FBS + 5% neutral red in 2× EMEM was added to the wells. The plates were again incubated for 18–24 h (RVFV) before counting or for 48 h with further 24–72 h incubation at room temperature (CCHFV) before counting.

2.4. Cellular cytotoxicity and measurement of EC_{50} and SI_{50} values

Compound toxicity was assessed for Vero E6 cells with the MTS-based assay, CellTiter 96® AQueous One Solution Cell Proliferation Assay (Promega, Madison, WI). Vero E6 cells were seeded in 96-well plates at a density of 20,000 cells/well in 100-μL of a complete DMEM and incubated overnight at 37 °C with 5% CO2. The next day medium was discarded and replaced with the compound containing medium. Compounds (10 mg/mL stock solution in DMSO) were serially diluted twofold from an initial starting concentration of 200–1.5 μg/mL in triplicate. EC_{50} and IC_{50} values were calculated based on fitting of the dose response curves of the virus-infected and uninfected, drug-treated cells using SigmaPlot. SI_{50} values were calculated from IC_{50}/EC_{50}.

2.5. Determination of the effect of drug treatment on production of viral RNA

To measure the levels of viral RNA within the cell in the presence of drug or mock controls, we used a real-time RT-PCR targeting the S segment vRNA as described previously (Chung et al., 2007). Briefly, total RNA from infected cell was extracted with TRIzol (Invitrogen) and 0.5 μg of total RNA was subjected to a reverse transcription reaction. The synthesized cDNA was used for a real-time RT-PCR assay as well as a mutation frequency assay (Sun et al., 2007; Chung et al., 2007). Mutation frequencies were calculated for each sample by comparing individual cDNA sequences with the published consensus sequences as described (Chung et al., 2007). Ninety individual cDNAs were analyzed for each treatment.

2.6. Dosing of inhibitors or guanosine

Guanosine was added to the culture medium in the presence of ETAR to address the ability of guanosine to reverse the effect of ETAR on HTNV. HTNV was added to Vero E6 cell for 1 h as described above, and media was replaced with a complete medium with or without 35 μM of guanosine combined with various concentration of ETAR (0, 44, and 89 μM). For the time of addition experiment, compounds were directly added into cell supernatant at the denoted time points. The effect of these treatments was evaluated with either a focus forming unit assay or real-time RT-QPCR as compared to the control group.

2.7. Measurement of intracellular ETAR metabolites and natural nucleotides

Confluent Vero E6 cells prepared as above for the antiviral studies were incubated at 37 °C with [^{3}H]ETAR, which was obtained from Moravek Biochemicals (Brea, CA). The purity of [^{3}H]ETAR was checked by using reverse phase HPLC prior to use in these studies.

H-5b). ^{13}C NMR (CD_3OD, 400 MHz) δ148.4, 145.6, 93.9, 86.9, 80.3, 75.0, 76.5, 71.6, 62.8. LCMS (ESI) *m/z*: calcd. for $C_9H_{11}N_3O_4$ $[M+1]^+$ 226.07, found 226.08.

The column used for purification was a 5 μm, 150 mm × 4.6 mm BDS Hypersil C-18 column (Thermo Electron Corp., Bellefonte, PA), and the mobile phase was 1.25% acetonitrile in 25 mM ammonium dihydrogen phosphate buffer (pH 4.5) for 30 min at a flow rate of 1 mL/min. ETAR eluted at approximately 14 min. Intracellular ETAR metabolites and natural nucleotides (ATP and GTP) were measured using strong anion exchange HPLC as described (Sun et al., 2007). The natural nucleotides (ATP and GTP) were detected by measurement of the UV absorbance at 260 nm, and radioactive metabolites of ETAR were detected by counting 1-min fractions. Intracellular ATP levels were used as a measure of the number of cells. None of the treatments shown in the current work resulted in changes to ATP levels. The radioactive fractions that eluted in the triphosphate region of the SAX HPLC were neutralized with 1 M NaOH and treated with 100 units of alkaline phosphatase (Promega) overnight at room temperature. The samples were subjected to reverse HPLC as described above to verify the identity of the nucleoside portion of the molecule.

2.8. Determination of antiviral activity in suckling mice

ICR suckling mice (Harlan, Prattville, AL) were used for all animal studies and were individually identified by tattoo. Pregnant mice were single housed with their pups in solid-bottom polycarbonate cages on stainless steel racks in an environmentally monitored, well-ventilated room maintained at a temperature of 18–26 °C, a relative humidity of 30–70%, and 12 h light/day. Bedding (P.J. Murphy Forest Products, Inc.; Montville, NJ) was used in the bottom of the cages. Dams were fed on Certified Rodent Diet #5002 (PMI Feeds Inc., St. Louis, MO) and tap water (City of Birmingham) provided ad libitum during the study periods. Procedures used in this study were designed to conform to accepted practices and to minimize or avoid causing pain, distress, or discomfort in the animals, and approved by the Institutional Animal Care and Use Committee (IACUC) at Southern Research.

Newborn were monitored for a 26-day period following intraperitoneal (ip) challenge with HTNV (strain 76-118) (Table 1). On Day 0, each mouse in Group 1 received 10 μL DMEM and each mouse in Groups 2–5 received 10 μL of 1×10^3 pfu HTNV diluted in DMEM media. Beginning on post-natal day 11 (PND11) (Day10), each mouse was treated with ETAR or ribavirin (MP Biomedical Inc.) via the ip route at 5 μL/g bodyweight for 15 days. All mice were observed twice daily throughout the study period for signs of morbidity and mortality, and detailed observations, including body weights, were recorded for all animals were obtained daily beginning on Day 1 p.i.

Table 1
Analysis of mutations of HTNV vRNA in the presence or absence of ETAR

	Placebo-treated	ETAR 10 μg/mL
Analyzed nucleotides	111,510	111,510
No. of cDNAs examined	90	90
Mutated nucleotides	19	17
Average mutation frequency (per 10,000)	1.7	1.5
% of cDNAs with mutations	17.8%	17.8%
% of C → U or G → A in total mutation	42.1%	29.4%
C → T mutations per 10,000 nt	0.4	0.2
G → A mutations per 10,000 nt	0.4	0.3
Mutation type		
Point		
Transition	11	9
Transversion	5	7
Amino acid change		
Missense	9	9
Nonsense	0	1
Silent	3	5
Frame shift	3	1

2.9. Statistical analysis

All statistical analyses were performed using SAS 9.1.3 program (SAS Institute). Mean to Death Days (MTDD) plus SD data were estimated using Kaplan–Meier Method. The Kaplan–Meier survival curves were compared by both log–rank test and Wilcoxon test. Both tests were adjusted for censored or surviving animals in the treatment groups. The survival curves from two different groups are significantly different if the *p*-values from both tests are lower than 0.0125 (the alpha = 0.0125 used was an adjusted alpha from the overall significant level of 0.05).

3. Results

3.1. Single concentration screening identified ETAR from a series of 3-substituted 1,2,4-triazole-β-ribosides

A series of triazole nucleoside analogs were tested at a single concentration of 30 μM for 3 days in cells infected with HTNV, ANDV, CCHFV or RVFV (data not shown). The supernatant from the Day 3 time point was analyzed for the level of infectious virus by plaque assay or a focus forming unit (FFU) assay. The antiviral activities were defined relative to untreated (virus only) and the positive control, RBV (61 μM). Among the compounds examined, ETAR (Fig. 1) inhibited ANDV and HTNV FFU by 98% and 94.3%, respectively. CCHFV showed a modest reduction in PFU (0.6 logs), however, ETAR did not demonstrate any activity against RVFV. In this assay, HTNV-infected Vero E6 cells treated with 6.25 μM MPA or 60 μM RBV showed 94% and 99% reduction in FFU, respectively (0.9 and 1.6 log decrease).

3.2. Dose response of ETAR with HTNV and ANDV

The anti-HTNV activity of ETAR was assessed from 8.9 to 89 μM using the FFU assay (Fig. 2A) and a real-time RT-PCR assay for HTNV RNA (Fig. 2B). In contrast to the effect of drug on vRNA levels, which did not show any significant reduction past 20 μM (Fig. 2B), there was a good dose response with ETAR with respect to the level of the infectious virus (FFU). The EC_{50} value for ETAR for HTNV was calculated to be 27 μM with a cell-based ELISA assay (data not shown). For comparison, MPA had an EC_{50} value of 67 μM using the same assay. The EC_{50} values for HTNV and ANDV with FFU assay were 10 μM and 4.4 μM, respectively (Fig. 2A). We used an MTS-based cytotoxicity assay to measure the toxicity of ETAR to Vero E6 cells and did not detect any toxicity up to a concentration of 880 μM. Because Vero E6 cells are a nonproliferating cell culture model, the cytotoxicity of ETAR was also determined against CEM cells, which are a rapidly proliferating human T-cell line. The concentration of ETAR required to inhibit the growth of CEM cells by 50% during a 72 h period was 7 ± 0.3 μM ($N = 3$). The concentration of RBV that inhibited the growth of CEM cells was approximately 50 uM (data not shown), which indicated that ETAR was a more potent inhibitor of CEM cell growth than was RBV.

3.3. Metabolism of ETAR in Vero cells

Because of the potent antiviral activity of ETAR, tritium labeled ETAR was obtained and its metabolism was evaluated in confluent Vero E6 cell cultures. The major intracellular metabolite eluted from SAX HPLC with a retention time of approximately 30 min, which was similar to that of ATP. Therefore, this metabolite has been tentatively identified as ETAR-5′-triphosphate (ETAR-TP). As indicated in Fig. 3, ETAR-TP reached its maximum level at about 3.4 pmol/nmol

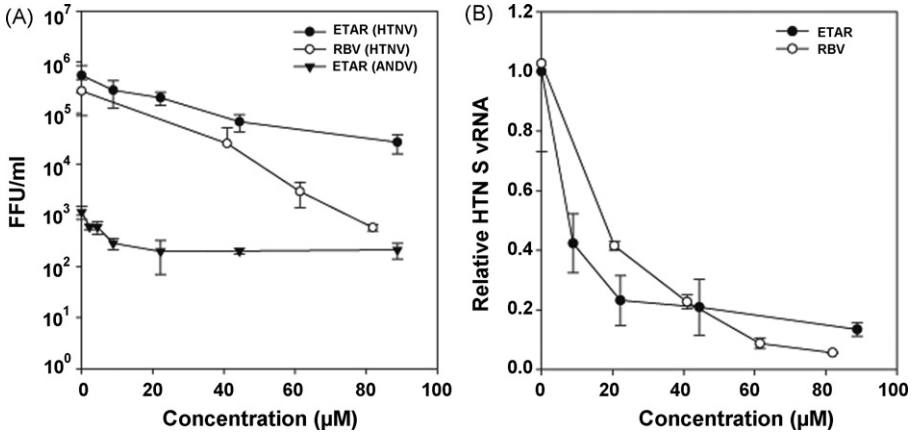

Fig. 2. Dose response of ETAR in Vero E6 cells infected with HTNV or ANDV. Vero E6 cells were infected with either HTNV (open or solid circle) or ANDV (reverse triangle) virus at a moi of 0.1 and cultivated in the presence or absence of RBV or ETAR for 72 h. The supernatant was harvested and subjected to FFU assay (A) or real-time RT-PCR (B). Data represent the means ± standard deviation from two independent experiments.

of ATP after 24 h treatment with 42 μM ETAR. The intracellular concentration of ETAR-TP was 2.4 and 2.7 pmol/nmol of ATP after 48 and 72 h of treatment, respectively. Since the intracellular concentration of ATP is approximately 3 mM, these results indicated that the intracellular concentration of ETAR-TP was approximately 10 μM at its peak after 24 h of treatment with 42 μM ETAR (Fig. 3A).

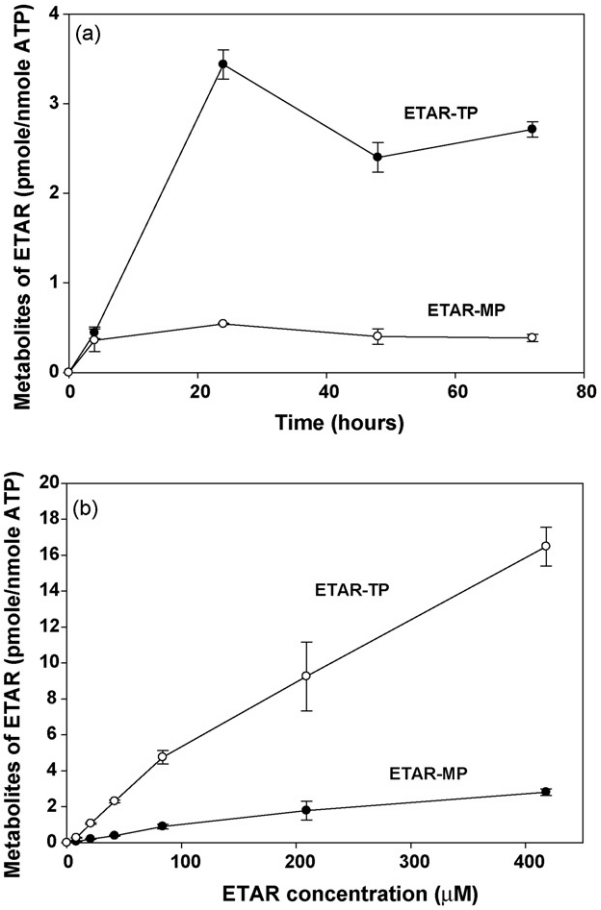

Fig. 3. Metabolism of ETAR in Vero E6 cells. Vero E6 cells were treated with either 42 μM [^{3}H]ETAR for 0, 4, 24, 48, and 72 h (Panel A) or 8, 21, 42, 84, 210, or 420 μM [^{3}H]ETAR for 24 h (Panel B). Acid-soluble extracts of the cell pellets were analyzed by strong anion exchange (SAX) HPLC to determine the intracellular amounts of ETAR-MP, ETAR-TP, and ATP. Each number represents the mean ± standard deviation from three measurements.

Increasing the extracellular concentration from 42 to 420 μM, resulted in an almost sevenfold increase in intracellular levels of ETAR-TP (Fig. 3B), which indicated that the metabolism of ETAR was not saturated in Vero cells up to a concentration of 420 μM.

A radioactive peak was also detected in the monophosphate region of the chromatogram. Because this peak comigrated with an ETAR-MP standard that was produced by incubating ETAR with adenosine kinase, it is likely that this metabolite is ETAR-MP. After 4 h of incubation the concentration of ETAR-MP was approximately the same as ETAR-TP. However, with increasing time the concentration of ETAR-TP, but not ETAR-MP, continued to increase. No other peaks of radioactivity were detected in the cell extracts.

Incubation of 10 μM RBV or ETAR with human adenosine kinase resulted in specific activities of 2900 or 230 nmol/(mg h), respectively (data not shown). The difference in specific activity of these two agents was similar to the difference in the rate of phosphorylation seen in Vero E6 cells. Since RBV is primarily metabolized by adenosine kinase, these results suggest that adenosine kinase was also responsible for the activation of ETAR in Vero E6 cells. In order to confirm that adenosine kinase is responsible for ETAR metabolism, Vero E6 cells were treated with 10 μM of iodotubercidin (a potent inhibitor of adenosine kinase activity) plus ETAR. Iodotubercidin inhibited the formation of ETAR-TP by 88% (data not shown), which indicated that adenosine kinase is the primary enzyme involved in the metabolism of ETAR in Vero cells.

3.4. Effect of ETAR on GTP levels in Vero E6 cells

Treatment of Vero E6 cells for 24 h with 42 μM ETAR caused intracellular GTP levels to decline by 60% (Fig. 4A). Addition of 10 μM iodotubercidin to cells incubated with ETAR prevented the decrease in GTP levels caused by ETAR (data not shown), which indicated that a metabolite of ETAR was responsible for the depression of GTP levels. Increased concentrations of ETAR did not result in a greater decline in intracellular GTP levels (Fig. 4B). The effect of ETAR on GTP levels was directly compared with that of RBV. In this experiment, incubation with 42 μM ETAR for 4 h resulted in a reduction of GTP levels of 79%, whereas incubation with 42 μM RBV for 4 h resulted in a reduction of GTP levels of 47%, which was similar to previous results (Sun et al., 2007).

3.5. Effect of guanosine on antiviral activity of ETAR

Previously, we have shown that the anti-HTNV activity of MPA was reversed by addition of exogenous guanosine, but that of RBV was not (Sun et al., 2007). To explore whether the antiviral activ-

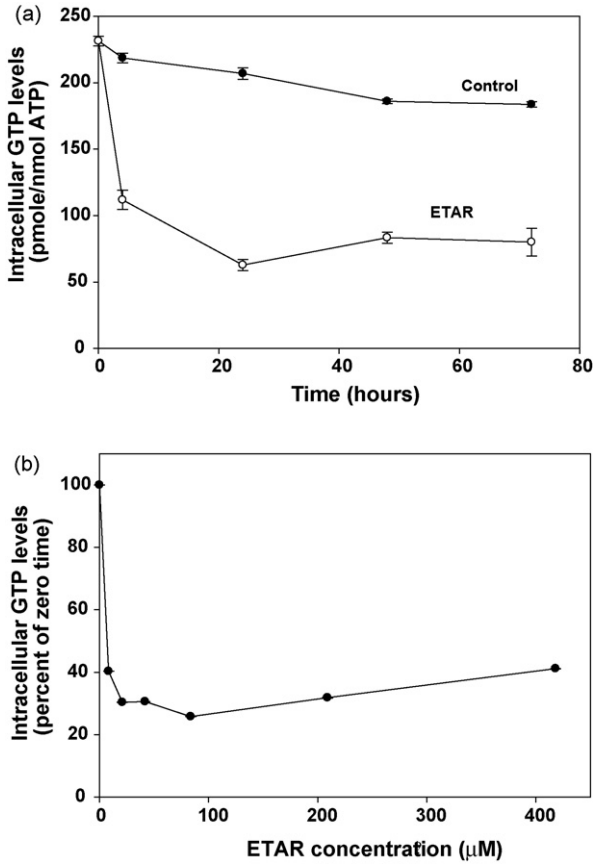

Fig. 4. Effect of ETAR on intracellular GTP levels in Vero E6 cells. Vero E6 cells were treated with either 42 μM [^{3}H]ETAR for 0, 4, 24, 48, and 72 h (Panel A) or 8, 21, 42, 84, 210, or 420 μM [^{3}H]ETAR for 24 h (Panel B). Acid-soluble extracts of cell pellets were analyzed by strong anion exchange (SAX) HPLC to determine intracellular GTP and ATP concentrations. The intracellular GTP level for untreated cells was 204 pmol GTP/nmol ATP. Each number represents the mean ± standard deviation from three measurements.

ity of ETAR was due to GTP reduction, HTNV-infected Vero E6 cells were incubated with a complete DMEM with ETAR in the presence or absence of 35 μM guanosine. After a 3-day treatment course, we measured HTNV FFU and vRNA (Fig. 5). In both assays, the addition of exogenous guanosine only partially reversed anti-HTNV activity (Fig. 5A) as reflected in viral RNA levels which were 70% of the untreated control (virus alone) (Fig. 5B). This implies that the antiviral effect of ETAR was primarily due to a decrease in GTP and hence suggests it targets IMPDH. However, the lack of recovery of the vRNA suggests that lower GTP levels alone are not the sole reason for its antiviral activity.

3.6. ETAR treatment does not cause increase in mutation frequency

Previously, we have shown that RBV promotes error replication of the HTNV genome (Chung et al., 2007; Severson et al., 2003). Since ETAR's structure is a derivative of RBV, we asked whether ETAR could cause an increase in mutation frequency. Compared to the placebo-treated HTNV group, there was no significant change in mutation frequency (Table 1) ($P > 0.05$ Student's t-test).

3.7. Profiling of the time of addition of ETAR to identify possible mechanism of action

A time of addition experiment was carried out to characterize the anti-hantaviral activity of ETAR. After infection of Vero E6 cells with either HTNV or ANDV RBV (82 μM), MPA (6.2 μM) or ETAR (89 μM) was added at 0, 8, 16, 24 and 32 h post-infection. The supernatants were harvested at 72 h post-infection and progeny virus levels were determined by FFU and compared with the non-treated control sample (Fig. 6). For both HTNV and ANDV, the level of antiviral activity with MPA did not change over time (60–83%). ETAR and RBV for HTNV (Fig. 6A), however, showed a different pattern from that of MPA. Anti-HTNV activity of these two drugs was more potent when it was added earlier than 16 h post-infection (95.1%, 91.5%, 81.5% inhibition for ETAR addition at 0, 8 and 16 h post-infection, respectively). This pattern of inhibition was similar for ANDV (Fig. 6B); however, ANDV differed in that it did not show saturation of its activity even at 32 h post-infection.

3.8. HTNV challenge of suckling mice with treated with RBV and ETAR

To evaluate the anti-viral efficacy of ETAR in an animal model, we made a preliminary assessment of toxicity over a range of ETAR concentrations in suckling mice. Clinical symptoms were assessed daily and hematology was assessed at Days 0 and 15. The dose of ETAR was adjusted daily according to the actual weight of the mouse. Mice at post-natal Day 10 (PND10) were injected with ETAR at 12.5, 50, and 100 mg/kg for 15 days intraperitoneally. ETAR showed no apparent clinical symptoms or abberant hematology in suckling mice when treated at 12.5 mg/kg for 15 consecutive days *in vivo*.

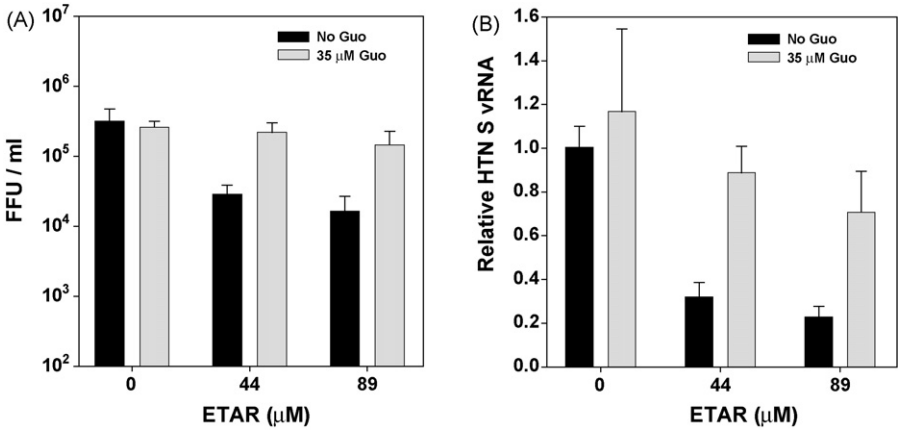

Fig. 5. Guanosine effect on ETAR anti-HTNV activity. HTNV infected cells were incubated with ETAR in the presence or absence of 35 μM guanosine. Progeny virus (A) or vRNA (B) was measured.

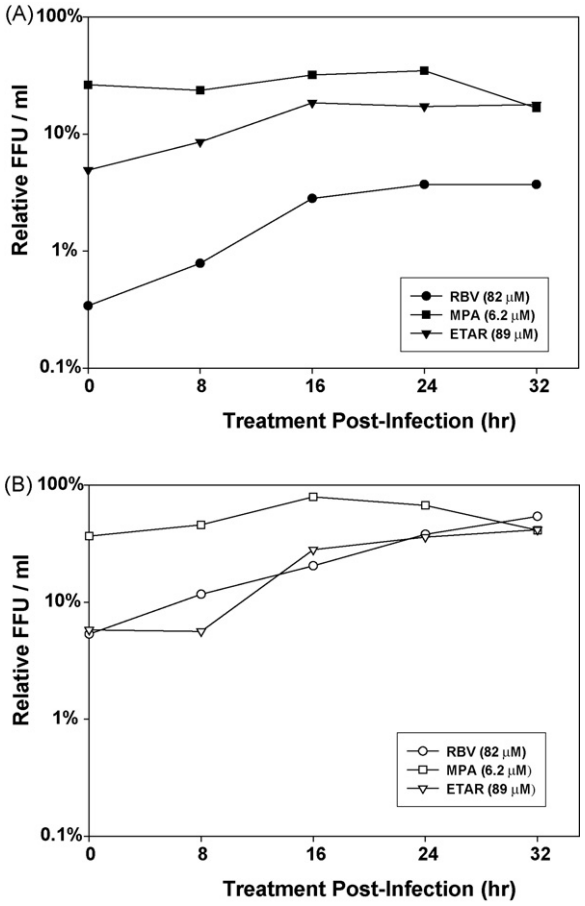

Fig. 6. Time-of-addition experiment for HTNV (A) and ANDV (B). After virus was adsorbed to cells for 1 h, residuals were removed, cells were washed and replenished with fresh culture media. Drug compounds were added at 0, 8, 16, 24 and 32 h post-infection ($T = 0$). Seventy two hours after infection, cell supernatants were harvested and the released progeny viruses were measured by a focus forming unit assay. The relative FFU was calculated by the comparison with FFU of mock treated control and that of experimental samples.

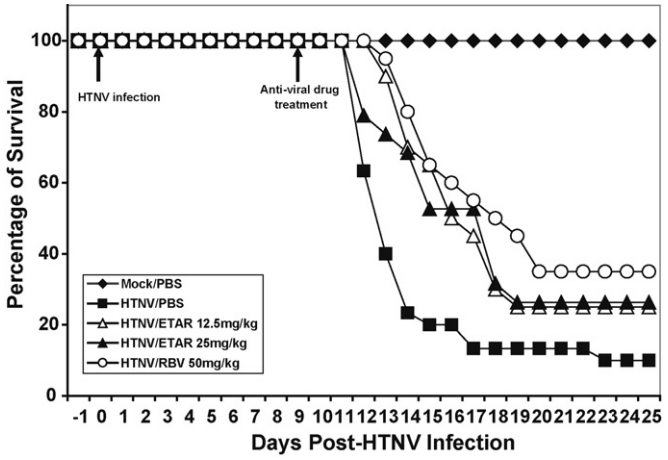

Fig. 7. In vivo antiviral activity of ETAR. Suckling mice were infected with 1000 pfu of HTNV on PND1. Each mouse was treated with anti-viral drugs (ETAR or ribavirin) from PND11 and continued for 14 consecutive days. Signs of morbidity and mortality were observed and recorded twice daily throughout the study periods for 26 days.

However, when suckling mice were treated with ETAR at 50 mg/kg and 100 mg/kg for 15 consecutive days, a 20% mortality resulted in both treatment groups. The clinical symptoms of these animals included loss of appetite, poor groom, hunched posture, and squinting. Clinical hematology assessment revealed that treatment with ETAR resulted in significant decreases in red blood cells and significant increases in platelets in both the 50 and 100 mg/kg treatment groups.

Based on these preliminary toxicity profiles, we selected 12.5 and 25 mg/kg doses of ETAR to treat suckling mice that were challenged with HTNV. RBV was included at 50 mg/kg as a positive control. Fig. 7 shows the survival curve for anti-viral drug treatment starting at PND10, when virus was present in all tissues according to our previous experience and that of others (Huggins et al., 1986). When mice were challenged with HTNV with no anti-viral drug treatment (PBS treatment), only 10% of the mice survived with a MTD of 15.5 ± 0.7 days. The MTD and percent survival were significantly higher in all the anti-viral drug treatment groups. RBV-treated mice showed 35% survival and a MTD of 18.5 ± 0.6 days. The MTD and percent survival were 17.5 ± 0.5 days and 25% for 12.5 mg/kg ETAR, and it was17.1 ± 0.7 days and 26% for the 25 mg/kg ETAR treatment group (Table 2). There were no significant differences in either the MTD or percent survival in mice treated with 12.5 mg/kg ETAR, 25 mg/kg ETAR or 50 mg/kg RBV.

4. Discussion

RBV exhibits broad-spectrum antiviral activity, *in vitro* and *in vivo*, against several families of DNA and RNA viruses, including Flaviviruses, Orthomyxoviruses, Paramyxoviruses and Reoviruses (Graci and Cameron, 2006). Multiple mechanisms of action have been implicated (Browne, 1979; Eriksson et al., 1977; Goswami et al., 1982; Malinoski and Stollar, 1981). These mechanisms include: (i) inhibition of IMPDH by 5′-monophosphate RBV leading to depletion of GTP pools; (ii) incorporation of RBV-TP into viral mRNA or vRNA resulting in replication and translation errors, some of them lethal; (iii) inhibition of viral RNA polymerase by RBV-TP; (iv) inhibition of viral or cellular guanylyl transferase activity by RBV-TP affecting viral mRNA cap formation; (v) modulation of the immune system. RBV is currently used in combination with pegylated interferon for the treatment of hepatitis C virus infection and has demonstrated varying success in the treatment of Lassa fever virus and respiratory syncytial virus infections. Clinical applications of RBV are adversely affected by dose-limiting hemolytic anemia, teratogenic effects, and reproductive toxicity (Ferm et al., 1978; Narayana et al., 2002). RBV-induced anemia, is dose- and time-

Table 2
Summary of efficacy of ETAR in HTNV-suckling mouse model

Group	PBS/PBS	HTNV/PBS	HTNV RBV 50 mg/kg	HTNV ETAR 12.5 mg/kg	HTNV ETAR 25 mg/kg
Number of animals	20	30	20	20	19
Mean to death (day)	>0.26	15.47	18.5	17.5	17.11
Standard error	N/A	0.67	0.61	0.51	0.67
Surviving percentage	100	10.00	35.00	25.00	26.32
P-value when comparing with HTNV/PBS group					
Log–rank			0.0008	0.0054	0.0194
Wilcoxon			<0.0001	0.0004	0.0168

dependent, but is reversible after discontinuation of treatment (Harvie et al., 1996; Huggins et al., 1986). The identification of new synthetic derivatives of RBV that target one or more virus-specific processes may provide improved selectivity and more effective drugs to treat these viral diseases.

ETAR was identified as a potent and selective agent against various (−)RNA viruses using *in vitro* assays. Using the cell-based ELISA assay, the EC_{50} of ETAR was 27 μM, which was similar to the non-competitive reversible IMPDH inhibitor MPA (EC_{50} of 67 μM). Using the FFU assay, the EC_{50} values of ETAR for HTNV and ANDV were 10 and 4.4 μM, respectively. Compared to RBV (Chung et al., 2007), the anti-hantaviral effect of ETAR was more potent than RBV. ETAR was not toxic to Vero E6 cells up to a concentration of 880 μM.

We evaluated ETAR in the suckling mouse model with HTNV challenge. The *in vivo* anti-viral activity of ETAR at the 12.5 and 25 mg/kg doses was similar to that of 50 mg/kg RBV, which suggested that ETAR might be a more effective anti-viral drug against HTNV infection in suckling mice. Although there were some differences in the experimental design (different dose of virus; different route of administration of virus; different route of administration of RBV), our results with RBV in the suckling mouse model were similar to those seen by Huggins et al. (1986). Huggins has shown that when the suckling mice were treated with 50 mg/kg RBV at PND10, 55% of the suckling mice were protected from HTNV-challenge with a MTD greater than 75 days (Huggins et al., 1986). Our results showed that RBV at 50 mg/kg could rescue 35% of animals from HTNV infection with MTD of 18 days in a 26-day follow-up period (Table 2) and was comparable with the previous results (Huggins et al., 1986). The maximal tolerated dose of ETAR in suckling mice (25 mg/kg) was lower than that of RBV (50 mg/kg).

The observation of the potent antiviral activity of ETAR, *in vitro* and *in vivo*, comparable to the efficacy of RBV, prompted further study to identify possible mechanisms resulting in antiviral effect. Both ETAR and RBV are representative of 3-substituted 1,2,4-triazole-β-ribosides, but exhibit altered steric and hydrogen bonding capacity. We recently demonstrated that the antiviral activity of RBV with HTNV was correlated with the production of RBV-TP and induction of mutations in the viral genome, while the inhibition of IMPDH was a secondary target (Sun et al., 2007). Using an analogous approach, we evaluated the metabolism and intracellular effects of ETAR. In contrast to our previous results that show RBV promotes mutation frequency of the HTNV genome (Chung et al., 2007; Severson et al., 2003), there was no significant change in mutation frequency with ETAR (Table 1). This is an expected result since even if ETAR is incorporated into the RNA, it lacks a pseudo-base pair capacity. ETAR, however, if incorporated could inhibit chain extension, and therefore would not be expected to induce mutations.

Physiologically relevant concentrations of phosphorylated ETAR metabolites were produced in Vero E6 cell cultures, with concentrations of ETAR-TP achieving maximum level after 24 h of treatment. The rate of metabolism of RBV was approximately 16-fold faster under identical conditions; however the final concentration of ETAR-TP was only fourfold lower than RBV-TP. ETAR-MP was also detected; however, its concentration did not increase significantly after 4 h of treatment. The NAD analog of ETAR was not observed under these conditions, but its possible presence at lower concentrations was not rigorously excluded. The rate of phosphorylation of ETAR by adenosine kinase was approximately 20-fold slower than for RBV, and paralleled the results observed in Vero E6 cells. The addition of the potent adenosine kinase inhibitor, iodotubercidin, significantly inhibited the formation of ETAR-TP, which indicates that adenosine kinase, the primary enzyme involved in the metabolism of RBV to RBV-MP, is also responsible for the initial phosphorylation of ETAR. Even though treatment of Vero E6 cells with ETAR did not affect the mutation frequency of HTNV viral RNA, it is possible, if not likely, that the inhibition of viral RdRp activity by ETAR-TP is primarily responsible for the antiviral activity of this compound. It is also possible that incorporation of ETAR-TP into viral RNA could lead to chain termination resulting in inhibition of further viral RNA synthesis. Furthermore, the fact that the metabolites of ETAR accumulate to lower concentrations in cells than those of RBV indicates that ETAR metabolites interact more potently with viral and/or human targets than do the metabolites of RBV.

Treatment of Vero E6 cells with ETAR caused GTP levels to decline by 60% and presents another possible mechanism for the observed antiviral activity. GTP levels were rescued by the addition of iodotubercidin, suggesting that a phosphorylated metabolite of ETAR was responsible for the observed depression of GTP. Inosine monophosphate dehydrogenase (IMPDH) is involved in the rate-determining step of *de novo* purine biosynthesis, and the ability of RBV-MP to inhibit IMPDH contributes to the pleiotropic antiviral phenotype of RBV. In order to evaluate GTP repression as a possible pathway for ETAR's antiviral activity, we incubated HTNV-infected Vero E6 cells with ETAR in the presence or absence of exogenous guanosine. Interestingly, the anti-HTNV activity was rescued by guanosine; however, the viral RNA levels remained repressed to 70% of untreated control. We have previously demonstrated that the anti-HTNV activity of MPA was totally reversed by the addition of guanosine (Sun et al., 2007). The observed incomplete guanosine reversal of HTNV viral RNA levels in ETAR-treated cells was similar to results using RBV, although the amount of reversal was different. These results suggest that reduction of GTP levels by inhibition of IMPDH contributed to the antiviral activity of ETAR, but was not the only operative mechanism. It is also possible that elevated GTP levels in cells treated with Guanosine (Sun et al., 2007) competed with the interaction of ETAR-TP and the viral polymerase, thereby interfering with the ability of this metabolite to inhibit viral RNA synthesis.

A variety of compounds capable of inhibiting IMPDH have been identified with broad spectrum antiviral activities. RBV-MP is capable of inhibiting IMPDH by competitive binding in the substrate site. Mycophenolic acid (MPA) is a noncompetitive, reversible inhibitor of IMPDH type I and II that binds to the NAD site. The nucleoside analog 5-ethynyl-1-β-D-ribofuranosylimidazole-4-carboxamide (EICAR) was designed as an irreversible inhibitor of IMPDH. EICAR is a substrate for adenosine kinase, and the resulting EICAR-MP metabolite inhibits IMPDH competitively and irreversibly by covalent alkylation of the electrophilic 5-alkynyl group with a critical cysteine sulfhydryl group. EICAR is also converted to the adenosine dinucleotide analog that inhibits IMPDH as an NAD analog, providing a cooperative inhibition of the enzyme leading to significant reduction in GTP levels. The 3-ethynyl moiety in ETAR metabolites is not expected to exhibit electrophilic properties and is therefore unlikely to undergo irreversible alkylation reactions analogous to EICAR. The corresponding EICAR-TP has also been postulated to act as a GTP analog capable of inhibiting a viral RNA polymerase (Minakawa et al., 1991; Balzarini et al., 1998).

We evaluated the cytotoxicity of ETAR against CEM cells, which are a human T-cell lymphoma cell line that replicate with a doubling time of approximately 30 h. ETAR had an IC_{50} of approximately 7 μM, and was not toxic to quiescent cells (Vero E6), but was cytotoxic to proliferating cells (CEM). It is likely that the inhibition of IMPDH activity by an ETAR metabolite and downstream depression of GTP levels is responsible for the cytotoxicity observed in proliferating CEM cells and the toxicity observed in the suckling mice.

Varying the time of addition of ETAR and MPA revealed additional differences in antiviral activity. MPA exhibited an ubiquitous antiviral effect for HTNV and ANDV replication regardless of when it was added, however, the antiviral activity of ETAR was maximized when it was added at 0 or 8 h after virus infection (HTNV and

ANDV, respectively). These results are consistent with inhibition of the IMPDH substrate-binding site by ETAR-MP as the primary mechanism for reduced GTP levels.

In conclusion, we report a novel, nucleoside analog which was active against an Old and a New World hantavirus. Mechanism and metabolism studies identified its activity was primarily due to IMPDH inhibition with reduction of GTP pools, which was combined with residual complementary activity possibly affecting the L protein. With its demonstrated efficacy in the suckling mouse model for HTNV, ETAR provides a promising scaffold for antiviral drug development.

Acknowledgments

This work was supported in part by NIH grant R21 AI064499-01 and a contract from the Department of Defense USAMRC W81XWH-04-C-0055 (PI Jonsson). We thank Ms. Feng Shuang at Southern Research Institute for statistical analyses. We thank Meredith James, Dana Skillman, Candi Looney, Donna Bowen, Robert Wood and Rodney Donaldson for technical support in the BSL3 animal studies.

References

Andrei, G., De Clercq, E., 1993. Molecular approaches for the treatment of hemorrhagic fever virus infections. Antivir. Res. 22, 45–75.

Balzarini, J., Stet, L., Matsuda, A., Wiebe, L., Knauss, E., De Clercq, E., 1998. Metabolism of EICAR (5-ethynyl-1-beta-D-ribofuranosylimidazole-4-carboxamide), a potent inhibitor of inosinate dehydrogenase. Adv. Exp. Med. Biol. 431, 723–728.

Bangash, S.A., Khan, E.A., 2003. Treatment and prophylaxis with ribavirin for Crimean-Congo Hemorrhagic Fever–is it effective? J. Pak. Med. Assoc. 53, 39–41.

Botten, J., Mirowsky, K., Kusewitt, D., Bharadwaj, M., Yee, J., Ricci, R., Feddersen, R.M., Hjelle, B., 2000. Experimental infection model for Sin Nombre hantavirus in the deer mouse (*Peromyscus maniculatus*). PNAS 97, 10578–10583.

Botten, J., Mirowsky, K., Ye, C., Gottlieb, K., Saavedra, M., Ponce, L., Hjelle, B., 2002. Shedding and intracage transmission of Sin Nombre hantavirus in the deer mouse (*Peromyscus maniculatus*) model. J. Virol. 76, 7587–7594.

Bronze, M.S., Greenfield, R.A., 2003. Therapeutic options for diseases due to potential viral agents of bioterrorism. Curr. Opin. Investig. Drugs 4, 172–178.

Browne, M.J., 1979. Mechanism and specificity of action of ribavirin. Antimicrob. Agents Chemother. 15, 747–753.

Chaparro, J., Vega, J., Terry, W., Vera, J.L., Barra, B., Meyer, R., Peters, C.J., Khan, A.S., Ksiazek, T.G., 1998. Assessment of person-to-person transmission of hantavirus pulmonary syndrome in a Chilean hospital setting. J. Hosp. Infect. 40, 281–285.

Chapman, L.E., Mertz, G.J., Peters, C.J., Jolson, H.M., Khan, A.S., Ksiazek, T.G., Koster, F.T., Baum, K.F., Rollin, P.E., Pavia, A.T., Holman, R.C., Christenson, J.C., Rubin, P.J., Behrman, R.E., Bell, L.J., Simpson, G.L., Sadek, R.F., Ribavirin Study Group, 1999. Intravenous ribavirin for hantavirus pulmonary syndrome: safety and tolerance during 1 year of open-label experience. Antivir. Ther. 4, 211–219.

Chung, D.H., Sun, Y., Parker, W., Arterburn, J., Bartolucci, A., Jonsson, C.B., 2007. Ribavirin reveals a lethal threshold of allowable mutation frequency for hantaan virus. J. Virol. 81, 11722–11729.

Compton, S.R., Jacoby, R.O., Paturzo, F.X., Smith, A.L., 2004. Persistent Seoul virus infection in Lewis rats. Arch. Virol. 149, 1325–1339.

De Clercq, E., 2005. Recent highlights in the development of new antiviral drugs. Curr. Opin. Microbiol. 8, 552–560.

Enria, D., Padula, P., Segura, E.L., Pini, N., Edelstein, A., Posse, C.R., Weissenbacher, M.C., 1996. Hantavirus pulmonary syndrome in Argentina. Possibility of person to person transmission. Medicina (B Aires) 56, 709–711.

Eriksson, B., Helgstrand, E., Johansson, N.G., Larsson, A., Misiorny, A., Noren, J.O., Philipson, L., Stenberg, K., Stening, G., Stridh, S., Oberg, B., 1977. Inhibition of influenza virus ribonucleic acid polymerase by ribavirin triphosphate. Antimicrob. Agents Chemother. 11, 946–951.

Ferm, V.H., Willhite, C., Kilham, L., 1978. Teratogenic effects of ribavirin on hamster and rat embryos. Teratology 17, 93–101.

Goswami, B.B., Crea, R., Van Boom, J.H., Sharma, O.K., 1982. 2′-5′-Linked oligo(adenylic acid) and its analogs. A new class of inhibitors of mRNA methylation. J. Biol. Chem. 257, 6867–6870.

Goundry, W.R.F., Baldwin, J.E., Lee, V., 2003. Total synthesis of cytotoxic sponge alkaloids hachijodines F and G. Tetrahedron 59, 1719–1729.

Graci, J.D., Cameron, C.E., 2006. Mechanisms of action of ribavirin against distinct viruses. Rev. Med. Virol. 16, 37–48.

Harvie, P., Omar, R.F., Dusserre, N., Desormeaux, A., Gourde, P., Tremblay, M., Beauchamp, D., Bergeron, M.G., 1996. Antiviral efficacy and toxicity of ribavirin in murine acquired immunodeficiency syndrome model. J. Acquir. Immune Defic. Syndr. Hum. Retrovirol. 12, 451–461.

Huggins, J.W., Hsiang, C.M., Cosgriff, T.M., Guang, M.Y., Smith, J.I., Wu, Z.O., LeDuc, J.W., Zheng, Z.M., Meegan, J.M., Wang, Q.N.<ET-AL, 1991. Prospective, double-blind, concurrent, placebo-controlled clinical trial of intravenous ribavirin therapy of hemorrhagic fever with renal syndrome. J. Infect. Dis. 164, 1119–1127.

Huggins, J.W., Kim, G.R., Brand, O.M., McKee Jr., K.T., 1986. Ribavirin therapy for Hantaan virus infection in suckling mice. J. Infect. Dis. 153, 489–497.

Kumarapperuma, S.C., Sun, Y., Jeselnik, M., Chung, K., Parker, W.B., Jonsson, C.B., Arterburn, J.B., 2007. Structural effects on the phosphorylation of 3-substituted 1-beta-D-ribofuranosyl-1,2,4-triazoles by human adenosine kinase. Bioorg. Med. Chem. Lett. 17, 3203–3207.

Lee, H.W., Lee, P.W., Baek, L.J., Song, C.K., Seong, I.W., 1981. Intraspecific transmission of Hantaan virus, etiologic agent of Korean hemorrhagic fever, in the rodent *Apodemus agrarius*. Am. J. Trop. Med. Hyg. 30, 1106–1112.

Lopez, N., Padula, P., Rossi, C., Lazaro, M.E., Franze-Fernandez, M.T., 1996. Genetic identification of a new hantavirus causing severe pulmonary syndrome in Argentina. Virology 220, 223–226.

Maes, P., Clement, J., Gavrilovskaya, I., Van Ranst, M., 2004. Hantaviruses: immunology, treatment, and prevention. Viral Immunol. 17, 481–497.

Malinoski, F., Stollar, V., 1981. Inhibitors of IMP dehydrogenase prevent sindbis virus replication and reduce GTP levels in *Aedes albopictus* cells. Virology 110, 281–289.

Martinez, V.P., Bellomo, C., San Juan, J., Pinna, D., Forlenza, R., Elder, M., Padula, P.J., 2005. Person-to-person transmission of Andes virus. Emerg. Infect Dis. 11, 1848–1853.

Mertz, G.J., Miedzinski, L., Goade, D., Pavia, A.T., Hjelle, B., Hansbarger, C.O., Levy, H., Koster, F.T., Baum, K., Lindemulder, A., Wang, W., Riser, L., Fernandez, H., Whitley, R.J., 2004. Placebo-controlled, double-blind trial of intravenous ribavirin for the treatment of hantavirus cardiopulmonary syndrome in North America. Clin. Infect. Dis. 39, 1307–1313.

Minakawa, N., Takeda, T., Sasaki, T., Matsuda, A., Ueda, T., 1991. Nucleosides and nucleotides. 96. Synthesis and antitumor activity of 5-ethynyl-1-beta-D-ribofuranosylimidazole-4-carboxamide (EICAR) and its derivatives. J. Med. Chem. 34, 778–786.

Narayana, K., D'Souza, U.J., Seetharama Rao, K.P., 2002. The genotoxic and cytotoxic effects of ribavirin in rat bone marrow. Mutat. Res. 521, 179–185.

Padula, P.J., Edelstein, A., Miguel, S.D., Lopez, N.M., Rossi, C.M., Rabinovich, R.D., 1998. Hantavirus pulmonary syndrome outbreak in Argentina: molecular evidence for person-to-person transmission of Andes virus. Virology 241, 323–330.

Peters, C.J., Simpson, G.L., Levy, H., 1999. Spectrum of hantavirus infection: hemorrhagic fever with renal syndrome and hantavirus pulmonary syndrome. Annu. Rev. Med. 50, 531–545.

Ramanathan, H.N., Chung, D.H., Plane, S.J., Sztul, E., Chu, Y.K., Guttieri, M.C., McDowell, M., Ali, G., Jonsson, C.B., 2007. Dynein-dependent transport of the Hantaan virus nucleocapsid protein to the endoplasmic reticulum-Golgi intermediate compartment. J. Virol. 81, 8634–8647.

Schmaljohn, C., Hjelle, B., 1997. Hantaviruses: a global disease problem. Emerg. Infect. Dis. 3, 95–104.

Schmaljohn, C.S., Hooper, J.W., 2001. Bunyaviridae: the viruses and their replication. In: Bernard, D.M.K., Fields, N., Bernard Roizman, Diane, E., Griffin, Malcolm, A., Martin, Robert, A., Lamb, Peter, M., Howley, Stephen, E., Straus (Eds.), Fields Virology, Vol.2. Lippincott Williams & Wilkins, Philadelphia, PA, pp. 1581–1633.

Schmaljohn, C.S., Hasty, S.E., Harrison, S.A., Dalrymple, J.M., 1983. Characterization of Hantaan virions, the prototype virus of hemorrhagic fever with renal syndrome. J. Infect. Dis. 148, 1005–1012.

Severson, W.E., Schmaljohn, C.S., Javadian, A., Jonsson, C.B., 2003. Ribavirin causes error catastrophe during Hantaan virus replication. J. Virol. 77, 481–488.

Sidwell, R.W., Huffman, J.H., Khare, G.P., Allen, L.B., Witkowski, J.T., Robins, R.K., 1972. Broad-spectrum antiviral activity of Virazole: 1-beta-D-ribofuranosyl-1,2,4-triazole-3-carboxamide. Science 177, 705–706.

Sun, Y., Chung, D.H., Chu, Y.K., Jonsson, C.B., Parker, W.B., 2007. Activity of ribavirin against Hantaan virus correlates with production of ribavirin-5′-triphosphate, not with inhibition of IMP dehydrogenase. Antimicrob. Agents Chemother. 51, 84–88.

Vitek, C.R., Breiman, R.F., Ksiazek, T.G., Rollin, P.E., McLaughlin, J.C., Umland, E.T., Nolte, K.B., Loera, A., Sewell, C.M., Peters, C.J., 1996. Evidence against person-to-person transmission of hantavirus to health care workers. Clin. Infect. Dis. 22, 824–826.

Wells, R.M., Young, J., Williams, R.J., Armstrong, L.R., Busico, K., Khan, A.S., Ksiazek, T.G., Rollin, P.E., Zaki, S.R., Nichol, S.T., Peters, C.J., 1997. Hantavirus transmission in the United States. Emerg. Infect. Dis. 3, 361–365.

Yanagihara, R., Amyx, H.L., Gajdusek, D.C., 1985. Experimental infection with Puumala virus, the etiologic agent of nephropathia epidemica, in bank voles (*Clethrionomys glareolus*). J. Virol. 55, 34–38.